Intermolecular Interaction in Carbon Nanotube Ropes

C. Thomsen (a), S. Reich (a), A. R. Goñi (a), H. Jantoljak (a), P. M. Rafailov[1]) (a),
I. Loa (b), K. Syassen (b), C. Journet (c), and P. Bernier (c)

(a) Institut für Festkörperphysik, Technische Universität Berlin, Hardenbergstraße 36,
D-10623 Berlin, Germany

(b) Max-Planck-Institut für Festkörperforschung, Heisenbergstraße 1,
D-70569 Stuttgart, Germany

(c) Groupe de Dynamique des Phases Condensées, Université Montpellier 2,
F-34095 Montpellier Cedex 5, France

Using Raman spectroscopy we determined the van-der-Waals component of the low-frequency vibration in ropes of single-walled nanotubes at 171 cm^{-1}. While Raman peaks in this frequency range are commonly believed to correspond to the pure radial breathing mode of a single tube, our pressure and temperature-dependent measurements show that van-der-Waals contribution of the peak observed at 514.5 nm excitation is necessary to explain its large pressure coefficient of 9.7 cm^{-1}/GPa. Our results are consistent with the small elastic modulus predicted for nanotube ropes.

Single-walled carbon nanotubes have moved into the center of scientific interest since their discovery in 1993 [1, 2]. Their one-dimensional structure formed by rolling up graphitic sheets to a long and narrow cylinder led to the anticipation of highly anisotropic electrical, optical and mechanical properties [3, 4]. Carbon nanotubes exist in single and multi-walled form, where the common preparation procedures for the former usually lead to formation of bundles of tubes, so-called nanoropes containing between 20 and 100 individual tubes [1, 2]. Calculations of the cohesive energy of such a nanotube crystal show that it is favorable to form a rope over retaining a free-standing tube by 10 to 25 meV per atom, the precise value depending on tube diameter [5].

Vibrational spectroscopy has become a widespread tool for the analysis of nanotubes [6 to 8]. Rao et al. have made a first assignment of observed peaks in the Raman spectra to mode symmetries. Strong features are usually found near 1590 cm^{-1} and near 170 cm^{-1} with peaks 10 to 100 times smaller in the intermediate frequency range (for excitation with $\lambda = 488$ or 514 nm). The high-energy structure usually consists of several closeby peaks assigned to A_{1g}, E_{1g} and E_{2g} mode symmetry, where neighboring carbon atoms vibrate out of phase in axial or tangential directions [6] (in the following tangential will refer to perpendicular to the axial and radial directions). The low-frequency mode is commonly referred to as the radial breathing mode, in which all carbon atoms of a single tube move in phase in radial direction; the eigenvector of such a mode should thus have the full symmetry of a single tube.

One approach for the calculation of nanotube vibrational frequencies is based on a zone-folding method which assumes little or no change of the elastic and vibrational

---

properties when rolling up a graphite sheet to a nanotube [9 to 12]. First-principles methods have been applied to the radial breathing mode by Kürti et al. [13] and to a series of Raman-active modes by Sánchez-Portal et al. [14]. The results agree mostly with those of the simple zone-folding methods showing that indeed curvature effects are small. A property of the radial breathing mode in particular is that its predicted frequency is proportional to the inverse of the nanotube radius, independent of the method of calculation. It is this common practice to take the frequencies in the low-energy region as an indication of the radius of the tubes present in a particular sample [15 to 17].

We show here that the frequency of the mode at 171 cm^{-1} in single-walled nanotubes has an unusually strong pressure dependence compared to the high-energy modes. This is attributed to a significant van-der-Waals interaction between the tubes within the nanoropes. The implications of this work are that conclusions based on the experimental determination of the nanotube diameter via the Raman frequency of the low-energy peak have to be reconsidered.

The single-walled carbon nanotubes used in the present study were as-grown samples prepared by the arc-discharge method. A metallic catalyst (4.2% Ni and 1.0% Y) provided the growth of about 80% nanotube ropes in the deposit around the cathode. Each rope contained about 20 nanotubes; for details we refer to [18]. Flakes of the nanotube material were cut into $100 \times 100 \, \mu m^2$ pieces and filled into a gasketed diamond anvil cell; using a 4:1 methanol–ethanol mixture as pressure medium we obtained pressures up to 10 GPa as determined by the ruby luminescence method [19]. The Raman spectra were recorded with a triple-grating spectrometer equipped with a charge coupled device (CCD) detector. The 488 and 514 nm lines of an Ar$^+$ and Kr$^+$ laser were used for excitation; all spectra were calibrated separately with neon or argon calibration lines; the resolution was 3 cm^{-1}.

In Fig. 1 we display the low-energy part of the Raman spectrum of single-walled nanotubes for various pressures. The position and width of the peak at near-atmospheric pressures are typical for this type of tubes and excitation at $\lambda = 514$ or 488 nm [17]. We find that the frequency shifts linearly with a pressure coefficient of 9.7 ± 0.5 cm^{-1}/GPa. The peak is also seen to broaden noticeably and to decrease in intensity. In Table 1 we compare the pressure coefficient of the low-energy mode with those found for the high-energy modes near 1593 cm^{-1} and those of graphite, which were taken from Ref. [20, 21]. The most striking result is that the mode at 171 cm^{-1} has a much larger pressure dependence than the high-energy modes of the nanotubes: we find a factor of 16 between the normalized quantities $\omega_0^{-1} \, d\omega/dp$, where p is the pressure. This implies that the elastic properties related to the low-energy vibration are much softer than one would expect were it a pure radial breathing mode of the nanotube. A similarly enormous difference between the elastic response in the in-plane direction compared to the out-of-plane direction is known from graphite when hydrostatic stress is applied (see Table 1). The factor of 50 between the pressure derivatives is understood in terms of the much weaker bonding between graphite planes (van-der-Waals bonding) than within the planes (covalent bonding) [20]. This difference suggests a significant contribution of a van-der-Waals type bonding for the vibrational eigenmode observed at 171 cm^{-1} in ropes of single-walled nanotubes. A similar van-der-Waals-force determined mode exists in graphite at 127 cm^{-1} as measured by neutron scattering [21]. Here the mode corresponds to a rigid c-axis displacement of the gra-

SWNT bundles

T = 300 K

λ_{exc} = 515 nm

Scattering Intensity (arb. units)

Frequency (cm^{-1})

200

190

180

170

9.7 cm^{-1}/GPa

0 1 2 3

Pressure (GPa)

0.2 GPa

0.7 GPa

1.2 GPa

1.8 GPa

2.5 GPa

4.1 GPa

150 200 250 300

Raman Shift (cm^{-1})
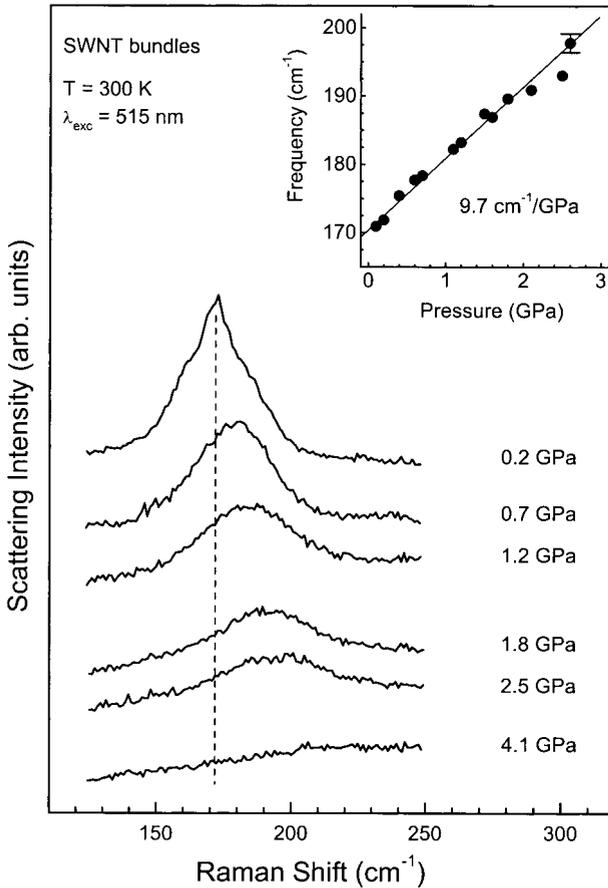
Fig. 1. Low-energy part of the Raman spectra of a single-walled nanotube bundle, a nanorope, under hydrostatic pressure and at 300 K. The inset shows the peak frequency as a function of pressure. The slope of the fitted line corresponds to a pressure coefficient of 9.7 ± 0.5 cm^{-1}/GPa

Table 1

The experimentally determined pressure and temperature coefficients of the most prominent peaks in the Raman spectra of single-walled nanotubes (SWNT) in comparison with those of graphite (Graph.). The temperature dependences of the SWNT were obtained by taking the full experimental shift between 20 and 300 K and dividing it by 280 K

ω_0 (cm^{-1})		$\omega_0^{-1} \, d\omega/dp$ (TPa^{-1})		elastic modulus (GPa)		γ		$-\omega_0^{-1} \, d\omega/dT$ (10^{-6} K^{-1})
SWNT	Graph.	SWNT	Graph.	SWNT	Graph.	SWNT	Graph.	SWNT
	44[a]		110[a]		36[a]		1.4[a]	
	127[b]		150[b]		36[a]		1.9	
171		57		33				55
1568	1579[a]	3.7	3.0[a]	880	1250[a]	1.09	1.06[a]	
1593		3.6		880		1.06		5.8

[a] Ref. [20].
[b] Ref. [21].

phite planes against each other. A pressure coefficient of $7\,\text{cm}^{-1}$/GPa for the low-energy mode in single-walled nanotubes has been reported recently and, based on a molecular-dynamics simulation, also explained by a van-der-Waals interaction [22]. The authors of Ref. [22] note that the additional interaction increases their mode frequency by $\approx 14\,\text{cm}^{-1}$. We analyze our results in terms of elasticity theory and arrive at a larger frequency increase due to the van-der-Waals term. This difference is partly due to the different experimentally determined pressure derivative and partly due to the hexagonal deformation of the tube cross section, which was observed in the molecular-dynamics calculation [22]. As we discuss later, our temperature-dependent measurements show that a deformation of the tube cross section cannot account for the large pressure derivative of the low-energy mode.

In order to investigate the frequency shift quantitatively, we derived the elastic properties of a single nanotube under hydrostatic pressure. We approximated the nanotube by a hollow cylinder with isotropic elastic properties within the sheet that is rolled up; the cylinder has a finite wall thickness and closed ends [23, 24]. In view of the similarity of the vibrational and elastic results of ab initio calculations compared to those not including curvature effects this approach is justified. We are thus able to determine the strain components $u_{ii} = \partial u_i/\partial x_i$ in axial, tangential and radial directions using the normal coordinates r, θ, and z,

$$u_{rr} = -\frac{pA}{E}\left(\nu^- - \nu^+\,\frac{R_1^2}{r^2}\right), \qquad u_{\theta\theta} = -\frac{pA}{E}\left(\nu^- + \nu^+\,\frac{R_1^2}{r^2}\right),$$

$$u_{zz} = -\frac{pA}{E}\,\nu^-\,, \tag{1}$$

where $A = R_2^2/(R_2^2 - R_1^2)$ with R_1 and R_2 are the inner and outer radius of the tube, ν is Poisson's ratio, $\nu^+ = 1 + \nu$, $\nu^- = 1 - 2\nu$, and E Young's modulus. The ratio of strain in tangential direction to that in axial direction is hence

$$\frac{u_{\theta\theta}}{u_{zz}} = 1 + \frac{1+\nu}{1-2\nu}\,\frac{R_1^2}{r^2}\,. \tag{2}$$

Using typical values for single-walled nanotubes (radius 6.9 Å, wall thickness 3.4 Å and Poisson's ratio $\nu = 0.14$ [14]) we find $u_{\theta\theta}/u_{zz} = 1.9$.

Given that the high-energy mode has an axial eigenvector a radial mode according to (2) should have a logarithmic pressure derivative about two times higher than the high-energy mode. We observe, however, a striking factor of 16, thus showing that the low-energy mode of Fig. 1 cannot be a pure radial breathing mode as is commonly assumed. Our conclusion does not depend much on the value of Poisson's ratio or Young's modulus.[2]) It can even be shown that the ratio in (2) varies only little if the ends of the nanotube are considered open.[3])

From the known properties of graphite we are able to give a quantitative estimate as to what fraction of the $171\,\text{cm}^{-1}$ mode is of van-der-Waals nature. Assuming simply additive force constants, we divide the logarithmic pressure derivative into a term originating from a pure radial breathing mode (index RBM) and a pure van-der-Waals

---

[2]) If the high-energy mode were tangential in its displacement the conclusion would hold even stronger.

[3]) This follows from an analogous analysis with the corresponding boundary conditions.

term (vdW),

$$\frac{\mathrm{d}\ln\omega_0}{\mathrm{d}p} = \left(\frac{\omega_{\mathrm{RBM}}}{\omega_0}\right)^2 \frac{\mathrm{d}\ln\omega_{\mathrm{RBM}}}{\mathrm{d}p} + \left(\frac{\omega_{\mathrm{vdW}}}{\omega_0}\right)^2 \frac{\mathrm{d}\ln\omega_{\mathrm{vdW}}}{\mathrm{d}p} \ . \tag{3}$$

Taking the pressure derivative of the RBM term to be that of the intramolecular high-energy graphite mode ($3.0\,\mathrm{TPa}^{-1}$, Table 1) and the van-der-Waals component to correspond to the pure van-der-Waals type B_{1g} mode of graphite ($150\,\mathrm{TPa}^{-1}$), we find the force constant of the mode at $171\,\mathrm{cm}^{-1}$ to be to 37% of van-der-Waals nature. Without van-der-Waals interaction, the mode frequency of the radial breathing mode would be $\omega_{\mathrm{RBM}} = 136\,\mathrm{cm}^{-1}$. If the intermolecular contribution were only twice as stiff, the van-der-Waals component of the $171\,\mathrm{cm}^{-1}$ mode would even increase to 75%.

The elastic properties of ropes or nanotube crystals have been calculated by Tersoff and Ruoff [5]. For a nanotube diameter of $D = 12\,\text{\AA}$ they find an equilibrium lattice
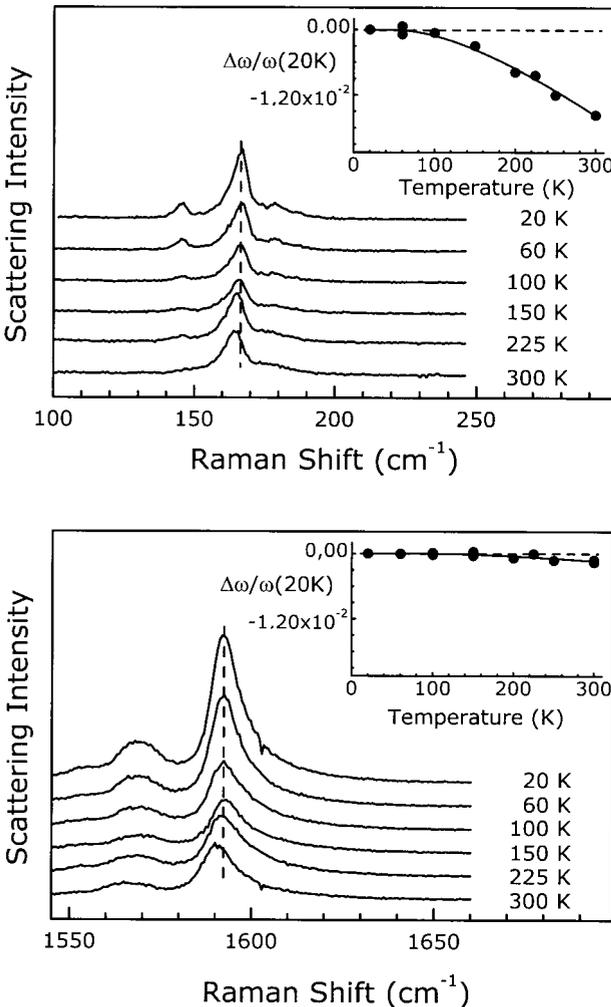
Fig. 2. Strongest low and high-energy peaks in the Raman spectra of single-walled carbon nanotubes measured at different temperatures and ambient pressure ($\lambda = 488$ nm). The insets show the relative frequency shift as a function of temperature

constant of $L = 15.4$ Å, a cohesive or formation energy of 18 meV per carbon atom and an elastic modulus for deformations in a plane perpendicular to the tube axes of $M = 34$ GPa. Parallel to the tube axes the elastic modulus is very high like in graphite when it is stressed in the in-plane directions. We can estimate the cross-sectional elastic modulus of the nanorope by taking the Grüneisen parameter of graphite perpendicular to the graphite plane ($\gamma = 1.9$) and find with d ln ω_0/dp of the 171 cm^{-1} mode

$$M = \gamma \left(\frac{\mathrm{d} \ln \omega_0}{\mathrm{d}p} \right)^{-1} \approx 33 \text{ GPa} \tag{4}$$

which is in excellent agreement with the value calculated for a nanorope.

For elastic moduli larger than $\approx$45 GPa Tersoff and Ruoff predicted a flattening of the tubes resulting in a hexagonal-like cross section [5]. To exclude this or other types of deformations as the cause for the large pressure coefficient of the 171 cm^{-1} peak we performed temperature-dependent measurements (Fig. 2). We find that the modes at 171 and 1593 cm^{-1} have a small but significant dependence on temperature in the range 20 to 300 K. Normalized to the absolute frequency, however, the low-energy mode is seen to be affected again much more strongly (Table 1). In general, a change in vibrational frequency with temperature is composed of an intrinsic term and one which results from the volume change due to thermal expansion. We thus find that the application of a uniform thermal stress to the nanorope produces − via thermal expansion − a similar effect on both modes as does pressure in the diamond anvil cell. This confirms that the observed changes cannot be ascribed only to deformations.

We thus conclude from the observed pressure and temperature dependences that the strongest low-frequency Raman peak at 171 cm^{-1} observed with 514 and 488 nm excitation cannot possibly be a pure radial breathing mode of an individual nanotube. Instead we have estimated an at least $\approx$40% van-der-Waals contribution to its force constant; the radial eigenvector is thus substantially mixed with displacements involving entire ropes.

References

[1] S. Iijima and T. Ichihashi, Nature (London) **363**, 603 (1993).
[2] D. S. Bethune, C. H. Kiang, M. S. de Vries et al., Nature (London) **363**, 605 (1993).
[3] See, e.g., A. Krishnan, E. Dujardin, T. W. Ebbesen, P. N. Yianilos, and M. M. J. Treacy, Phys. Rev. B **58**, 14013 (1998).
[4] J.-P. Salvetat, G. A. D. Briggs, J.-M. Bonard et al., Phys. Rev. Lett. **82**, 944 (1999).
[5] J. Tersoff and R. S. Ruoff, Phys. Rev. Lett. **73**, 676 (1994).
[6] A. M. Rao, E. Richter, S. Bandow et al., Science **275**, 187 (1997).
[7] U. Kuhlmann, H. Jantoljak, N. Pfänder, P. Bernier, C. Journet, and C. Thomsen, Chem. Phys. Lett. **294**, 237 (1998).
[8] M. S. Dresselhaus, G. Dresselhaus, and P. C. Eklund, Science of Fullerenes and Carbon Nanotubes, Academic Press, New York 1996 (p. 839).
[9] R. A. Jishi, L. Venkataraman, M. S. Dresselhaus, and G. Dresselhaus, Chem. Phys. Lett. **209**, 77 (1993).
[10] J. P. Lu, Phys. Rev. Lett. **79**, 1297 (1997).
[11] E. Richter and K. R. Subbaswamy, Phys. Rev. Lett. **79**, 2738 (1997).
[12] A. Charlier, E. McRae, M.-F. Charlier, A. Spire, and S. Forster, Phys. Rev. B **57**, 6689 (1998).

[13] J. KÜRTI, G. KRESSE, and H. KUZMANY, Phys. Rev. B **58**, R8869 (1998).
[14] D. SÁNCHEZ-PORTAL, E. ARTACHO, J. M. SOLER, A. RUBIO, and P. ORDEJÓN, Phys. Rev. B **59**, 12678 (1999).
[15] P. C. EKLUND, J. M. HOLDEN, and R. A. JISHI, Carbon **33**, 959 (1995).
[16] E. ANGLARET, J. L. SAUVAJOL, S. ROLS et al., Electronic Properties of Novel Materials, Progress in Molecular Nanostructures, Ed. H. KUZMANY, J. FINK, M. MEHRING, and S. ROTH, American Institute of Physics, Woodbury 1998 (p. 116).
[17] S. BANDOW, S. ASAKI, Y. SAITO et al., Phys. Rev. Lett. **80**, 3779 (1998).
[18] C. JOURNET, W. K. MASER, P. BERNIER et al., Nature (London) **388**, 756 (1997).
[19] G. J. PIERMARINI, S. BLOCK, J. P. BARNETT, and R. A. FORMAN, J. Appl. Phys. **46**, 2774 (1975).
[20] M. HANFLAND, H. BEISTER, and K. SYASSEN, Phys. Rev. B **39**, 12598 (1989).
[21] B. ALZYAB, C. H. PERRY, C. ZAHOPOULOS, O. A. PRINGLE, and R. M. NICKLOW, Phys. Rev. B. **38**, 1544 (1988).
[22] U. D. VENKATESWARAN, A. M. RAO, E. RICHTER, M. MENON, A. RINZLER, R. E. SMALLEY, and P. C. EKLUND, Phys. Rev. B **59**, 10928 (1999).
[23] See e.g. LANDAU and LIFSCHITZ, Lehrbuch der Theoretischen Physik, Bd. VII, Elastizitätstheorie, Akademie-Verlag Berlin 1991.
[24] C. THOMSEN, S. REICH, H. JANTOLJAK, I. LOA, K. SYASSEN, M. BURGHARD, G. S. DUESBERG, and S. ROTH, Appl. Phys. A, in print.